Trends and Spatial Patterns of 20th century Temperature, Rainfall and PET in the semi-arid Logone River Basin, Sub-Saharan Africa

Asmita Murumkar[1*], Michael Durand[1,2], Alfonso Fernández[3], Mark Moritz[4], Bryan Mark[1,5], Sui Chian Phang[6], Sarah Laborde[4], Paul Scholte[7], Apoorva Shastry[1,2], Ian Hamilton[6,8]

1. Byrd Polar and Climate Research Center, The Ohio State University, Columbus Ohio

2. School of Earth Sciences, The Ohio State University, Columbus Ohio

3. Department of Geography, Universidad de Concepcion, Chile

4. Department of Anthropology, The Ohio State University, Columbus Ohio

5. Department of Geography, The Ohio State University, Columbus Ohio

6. Department of Mathematics, The Ohio State University, Columbus Ohio

7. German Society for International Cooperation, Yaounde, Cameroon

8. Department of Evolution, Ecology and Organismal Biology, The Ohio State University, Columbus Ohio

*Corresponding email: murumkar.1@osu.edu

Abstract

Sub-Saharan floodplains are sensitive to climatic changes in their upstream drainage basin, a major concern is given the dependency of millions of people for their daily subsistence. Understanding hydroclimatic trends and variability is critical for developing integrated coupled human and natural system models to evaluate future scenarios of vulnerability. Here we describe the historical climatic changes in the Logone River basin using grid-based climatic data during a time of concomitant human hydrological modification of the floodplain. Temporal trends were analysed by comparing two periods i.e. 1901/1921-1961 (pre-1960) and 1961-2013 (post-1960). Trends were analysed spatially based on the basin's two Köppen climatic zones: savanna (Aw) covering the southern upstream areas and semi-arid hot (BSh) covering the northern downstream areas. The results show significant increasing trends in maximum and minimum temperatures and potential evapotranspiration (PET), and non-significant decreasing trends in annual rainfall and number of rainy days, across the study area. These climatic changes on temporal and spatial scales play an important role for the coupled natural and human systems in the Logone floodplain.

Highlights

- *Spatio-temporal climatic variations play an important role in flooding pattern*
- *Maximum/minimum temperatures of the Aw and BSh zones showed increasing trends*
- *Decreasing rainfall and increasing PET trends observed in the watershed*

- *Logone basin is getting warmer, impacting flooding pattern of the semi-arid region*
- *Hence, socioeconomic consequences increasingly impacted in the downstream of the basin*

Keywords: *hydro-climatic changes; climatic zones, Logone Floodplain, trends*

1. Introduction

The global average combined land and ocean surface temperature data show a warming of 0.85°C (0.65 to 1.06°C), over the period of 1880–2012 as calculated by a linear trend (Hartman et al. 2013). The change in temperature and rainfall have significant impact upon hydrological parameters, viz. runoff, evapotranspiration, soil moisture and groundwater (Goyal 2004). Nevertheless, it is not obvious how these temperature-sensitive hydroclimatic factors interact to impact net fluxes of regional water cycles (Milly et al. 2005), especially as temperature and rainfall are expected to show considerable spatial variability. For example, changes in evapotranspiration (ET) exhibit tremendous spatial variation (Abtew et al. 2011; Shadmani et al. 2012; Spinoni et al. 2017). The changes in hydrological parameters can have profound disruptive effects on water availability, floods, agricultural productivity and ecosystem at local and regional levels; analysis of hydroclimate data is thus imperative to understanding the pervasiveness of climate change (Savo et al. 2016).

The extensive floodplains in sub-Saharan Africa support human populations of millions. These floodplains become inundated when there is overbank flow from the river, a process that is well synchronized with the onset of the rainy season and recurs annually (Fernández et al. 2016). In many areas, traditional knowledge of the timing and spatial extent of this annual flooding season enables a relatively organized web of co-existing economic and social activities such as agriculture, fishing, and pastoralism (Acreman and Hollis 1996; Thompson and Polet 2000; Westra and De Wulf 2009). As these livelihoods are intimately dependent upon flooding, the potential impacts of climate change on the seasonality and extent of floods are a major concern across African floodplains (Mitchell 2013). Annual flooding is sensitive to spatial and temporal changes in rainfall and temperature, which drive processes like evapotranspiration and affect flood characteristics including timing, extent, and duration. Since the 1960s, temperatures in Africa have increased but with substantial regional variability in the magnitude of warming and rainfall (Boko 2007; Malhi and Wright 2004; Nicholson et al. 2000). Over southern and western Africa, there has been an increase in the number of warm spells (New et al. 2006). In the tropical rain-forest zone, declines in mean annual rainfall of around 4% in West Africa, 3% in North Congo and 2% in South Congo for the period 1960 to 1998 were noted (Malhi and Wright 2004) along with a 10% increase in annual rainfall along the Guinean coast (Nicholson et al. 2000). Decreasing rainfall is linked to decreasing agricultural production and reduced natural vegetation and threatens livelihoods dependent on them (Assan et al. 2009).

The Logone River floodplain in the Far North Region of Cameroon covers approximately 7,800 km^2 and provides vital socio-economic and environmental resources, supporting thousands of fishers, farmers and herders as well as globally important wildlife (Loth 2004; Scholte 2005). The socio-economy within the floodplain include pastoralism, agriculture, and fishing, and are influenced by seasonal flooding dynamics. For example, while full pastoralism season extends during the dry months over the inundated area, fishers have their peak season (bigger fishes) during the flooding season within the same sector (Loth et al. 2004). Since the 1960s, there has been an exponential growth of fishing canals and this reflects the increasing dependency on the floodplain by fishers (Laborde et al. 2016). Climatic changes along with hydrological structures and management have led to reductions in flooding over the past four decades and this has negatively impacted the inhabitants dependent on the flooding (Loth 2004; Scholte 2005). Floodplain fish production is driven by flooding patterns with a positive relationship between production and flood magnitude (Welcomme and Hagborg 1977), and changes in river hydrology threat freshwater fishing globally (Vörösmarty et al. 2010). Thus, the sustained wellbeing of the regional population presents a need to understand the impact of climate on flood patterns such as magnitude, timing and duration.

The 2007 Intergovernmental Panel on Climate Change (IPCC) described accelerated warming of the African continent since the 1960s (Boko et al. 2007). The low-latitude region (25ºN-25ºS) in which the Logone river basin falls has responded faster than other areas to global change (Mahlstein et al. 2011). Further, over the last half-century, there have been well-documented drought across the Sahel (1968-1997) and southern Africa with partial recovery in the early 21st century (Nicholson 2001; Christensen et al. 2007). Rainfall in the Logone basin and the West African monsoon are linked to the Congo River basin and the Walker circulation (Cook and Vizy 2015). These studies highlight the complex relationship between different climatic processes and floodplain dynamics. Indeed, addressing this complexity is a first step in understanding the regional sensitivity of flooding dependent livelihoods to the threat posed by climate change.

The Chari/Logone river system contributes approximately 90% of Lake Chad's water (Bastola and Francois 2012) which is a source to more than 30 million people (Leblanc et al. 2007). The Lake chad is very sensitive to rainfall and flow changes. Therefore, this study assesses the long-term climatic variation in the Logone River basin to better understand the effect of regional climate changes superimposed upon local disruptions to surface hydrologic processes important for floodplain livelihoods. An increase in anthropogenic activities, i.e. emission of greenhouse gases was observed globally during 1960-1990 (Kittel et al. 1995; Hulme et al. 1999). Most of the global climate models (GCMs) consider 1960-1990 as the baseline period for the projection of future climate scenarios due to availability of observational data and coverage during this period compared to earlier periods. Here we examine rainfall, number of rainy days to characterize the hydro-climatic variation over 113 years, whereas maximum-minimum temperature and potential evapotranspiration (PET) over 93 years from available gridded datasets, while accounting for the impact of increased anthropogenic activity starting in approximately 1960s. Evaluation of these variables can help unravel the effect of global climate changes coupled with local disruptions on regional surface hydrology. For example, small changes in the Logone watershed rainfall has historically produced large variations in the streamflow and annual flooding on the Logone floodplain (McDonald 1993). The floodplain has socio-ecological importance as explained earlier. The analysis of the climatic variability within these climatic zones will provide a more efficient manner for assessing the climatic-ecological changes in the basin. Therefore, we perform separate analyses for different climatic zones within the basin, different time periods (before and after 1960) and for the dry and rainy season, separately. The main objective of the study is to analyze the long-term climatic change in the Logone-Lake Chad basin to better understand the influence of the climatic variations in the hydrology of the basin. It will provide a baseline of hydroclimatic indicators of the current state of the Logone floodplain.

2. Study Area

The Logone River is a major tributary of the Chari River located in the Western Central African Republic, Northern Cameroon and Southern Chad (Fig. 1). The Pendé River (Eastern Logone) in the Central African Republic and the Mbéré River (Western Logone) at the East of Cameroon are the two major tributaries of the Logone. The total length of the Logone River is about 1000 km with a catchment area of 90,830 km^2.

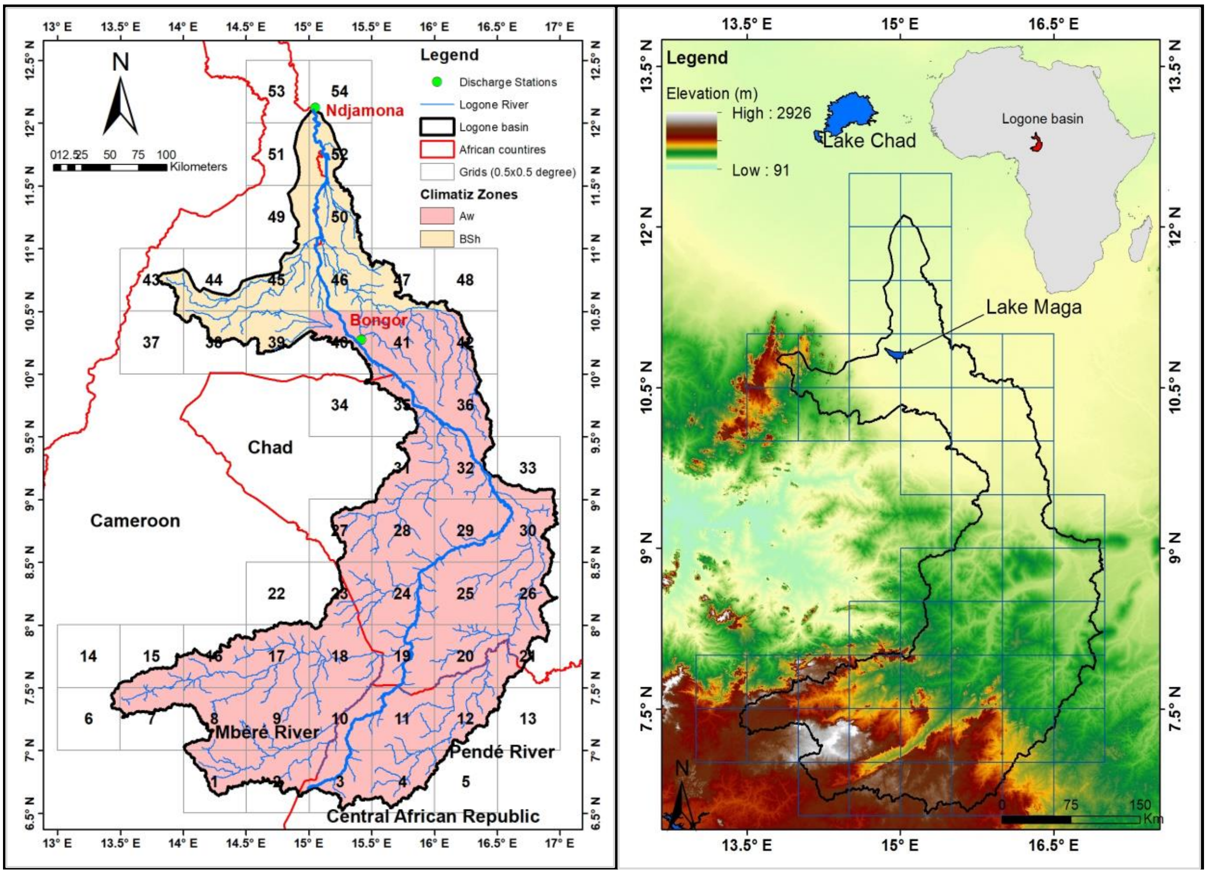

Fig. 1. Drainage and elevation map of the Logone river basin with nested grids of 0.5° x 0.5° resolution

The Logone watershed falls into two Köppen–Geiger climatic zones (Köppen 1900; Geiger 1954; Kottek et al. 2006): “Tropical wet and dry or Savannah climate” (Aw: upstream basin) and “Steppe climate (Semi-arid: downstream floodplain): Hot Steppe (BSh)”. The Aw climate is characterized by pronounced dry seasons, with the driest month having rainfall less than 60 mm and less than 1/25 of the total annual rainfall. The steppe climates (BSk and BSh) are intermediates between the desert and humid climates in ecological characteristics and agricultural potential. The upper (southern) basin is classified as Aw and the lower basin as BSh. The hydrological connectivity to Aw is crucial to the ecological vitality of the floodplain of the basin. The southern basin has a greater topographic variation (elevation range 2926 m to 330 m). The northern basin is relatively flat topography (elevation ranges from 330 m to 285 m) especially in the floodplain area in the far north. The Aw and BSh zones cover approximately 75,130 km^2 and 15,700 km^2 area of the basin, respectively.

The floodplain (located in grids 51 and 52, in Fig. 1) falls within the BSh climatic zone. According to available hydroclimatic records, the dry season extends from November to April, with more than 80% of year rainfall falling between July and September, average evaporation in excess of 200 mm/month, while temperatures remain above 22°C year-round (Fernández et al. 2016). When flooded as a result of seasonal flows of rainfall originating from the Aw zone, it serves as habitat for fishes to reproduce and grow as well as fertile land for growing rice. Following flood recession, the floodplain supports the growth of other crops and its vegetation serves as pastures for cattle and other livestock. The floodplain is populated by about 200,000 people on the Cameroonian side (Delclaux et al. 2010). There is a clear dependency on flooding to support the livelihoods of floodplain inhabitants.

The annual flooding of the floodplain is driven by patterns of local rainfall, runoff, and overbank flow from the Logone River (Delclaux et al. 2010). The floodplain experiences large evapotranspiration fluxes from the surface of open water and emergent vegetation. Potential evaporation in this region recorded as about 3m/year (Delclaux et al. 2010). The flooding is also driven by hydrology modifying engineering projects. These include the construction of Maga dam for rice production (Fig. 1), the use of flood defence embankments along the banks of the Logone River and construction of anthropogenic fish canals (Loth 2004; Scholte 2005; Laborde et al. 2016; Moritz et al. 2016). Overbank flow by the Logone River is the primary source for floodplain inundation (Delclaux et al. 2010). MacDonald (1993) investigated the relationship between rainfall and runoff of the upper Chari-Logone catchment area, i.e. the Aw zone, in Fig. 1. They concluded that (i) small changes in rainfall produced large variations in surface runoff, and (ii) two, or even only one year of above or below average rainfall resulted in multiple years with above or below average river flows. This shows how a short-term or small magnitude of climatic forcing may affect the long-term hydrologic behavior of the basin.

3. Data and Methods

We used the gridded dataset for analysis because of the low density and discontinuous instrumental records, the best option to better provide a baseline for studies on future hydroclimate in the region are gridded products. Among those, gridded products based on interpolation (such as Climate Research Unit) seems to be better qualified to represent the climatology of the region, given that reanalysis data is usually too short (e.g. ERA and MERRA), too coarse (e.g. NCAR NCEP). Fifty-four 0.5° x 0.5° resolution grid cells of the CRU dataset cover the entire Logone basin (Fig. 1). Fifteen of these grid cells fall in the BSh (northern downstream) zone, while 39 fall in the Aw (southern upstream) zone based on the long-term averages. The CRU TS 3.22 dataset is based upon more than 4000 weather stations globally. The monthly data set (0.5°x0.5°) includes the following climatic variables: mean, maximum and minimum temperatures; rainfall, number of rainy days, vapour pressure, potential evapotranspiration (PET) and cloud cover. The data were downloaded from Centre of Environmental Data Archival (http://badc.nerc.ac.uk). A detailed description of the datasets is given by Harris et al. (2014). Most data are available for the duration of 1901-2013. Using CRU fields implies certain smoothing of the climatology of the study area, but given this is a data-sparse region, few instrumental records are available to study long-term behavior and they are often discontinuous. This problem has led previous studies to use available gridded datasets, especially CRU (Mahmood et al. 2019). Mahmood and Jia (2018) suggested that the CRU data can be used with high confidence. We likewise attempted to compile all available records to perform validation of the CRU data, finding 6 stations that registered temperatures during the analysed period and 10 for rainfall, in both cases with discontinuous coverage (given in supporing documents; Table S1). Maroua station presented a continuous record during the whole studied period, but only for rainfall. All other records presented shorter records, with an average length of 40 years. However, this nominal length includes years with incomplete monthly coverage. Annual averages for temperatures and total sums for rainfall from instrumental observations were only calculated for years where all months had records, reducing the effective sample for comparison, especially for temperatures. Correlations between these observations and the corresponding CRU grid box are generally statistically significant at alpha=0.1, except for two temperature records, while the temperature bias mostly negative and small (within a degree); the highest bias is about $\pm$10% for rainfall considering that the annual rainfall of the grid is ~1000 mm (Fernández et al. 2016) (Table S1: refer calculated mean bias for rainfall and Fig. 2: grid-wise annual rainfall over the basin). We determined that some of the pre-1960 data appeared to contain artifacts, and therefore pre-1960 trend analyses were conducted using slightly different durations for each hydro-climatic parameter. We compare streamflow data at the Bongor station (1954-1995) to basin rainfall. The streamflow data are described in detail by Fernandez et al. (2016).

We analyzed temporal variation of climatic parameters (rainfall, number of rainy days, maximum and minimum temperatures, and potential evapotranspiration) of each grid in the basin using Mann Kendall (MK) test for non-auto-correlated and Modified Mann Kendall (MMK) test for auto-correlated series for trend detection (Anderson 1942; Mann 1945; Kendall 1955; Yue et al. 2002; Basistha et al. 2009), and Theil and Sen's slope estimator test (Theil 1950; Sen 1968) for estimation of the magnitude of trend slope. The significance of auto-correlation up to the lag-3 was found by Students's t-test (Cunderlik and Burn, 2004). The percent change over the mean was calculated using Theil and Sen's slope estimator. The significance of simple linear regression of annual climatic parameters of the climatic zones of the basin was analyzed using a *t*-test (Haan 1995). Trend analysis of streamflow at Bongor could not be performed due to lack of continuous data over a given time period.

Statistical significance of each trend was tested at the 10% significance level. Trend analysis of climatic data was performed for three durations: for the entire duration (1901/1921-2013), and for two partial durations: 1901/1921-1960 (pre-1960) and 1961-2013 (post-1960), which are intended to represent before and after accelerated anthropogenic activities, respectively. We also compute separate trends for different climatic zones within the basin, and for dry and rainy seasons. Note that for temperatures and PET, trends were computed beginning in 1921 due to data quality and availability issues.

4. Results

The spatial distribution of the climatic parameters across the basin is shown in Fig. 2. The rainfall and number of rainy days decreases from the upstream (south, Aw) to downstream (north, BSh) of the basin. Rainfall to the far south reaches 1550 mm/year, whereas in the north it reaches a minimum of 500 mm/year, over a factor of three less than in the headwaters. Temperature and PET increase from upstream to downstream of the basin, and also show large spatial variations of 6°C and 900 mm/year, respectively.

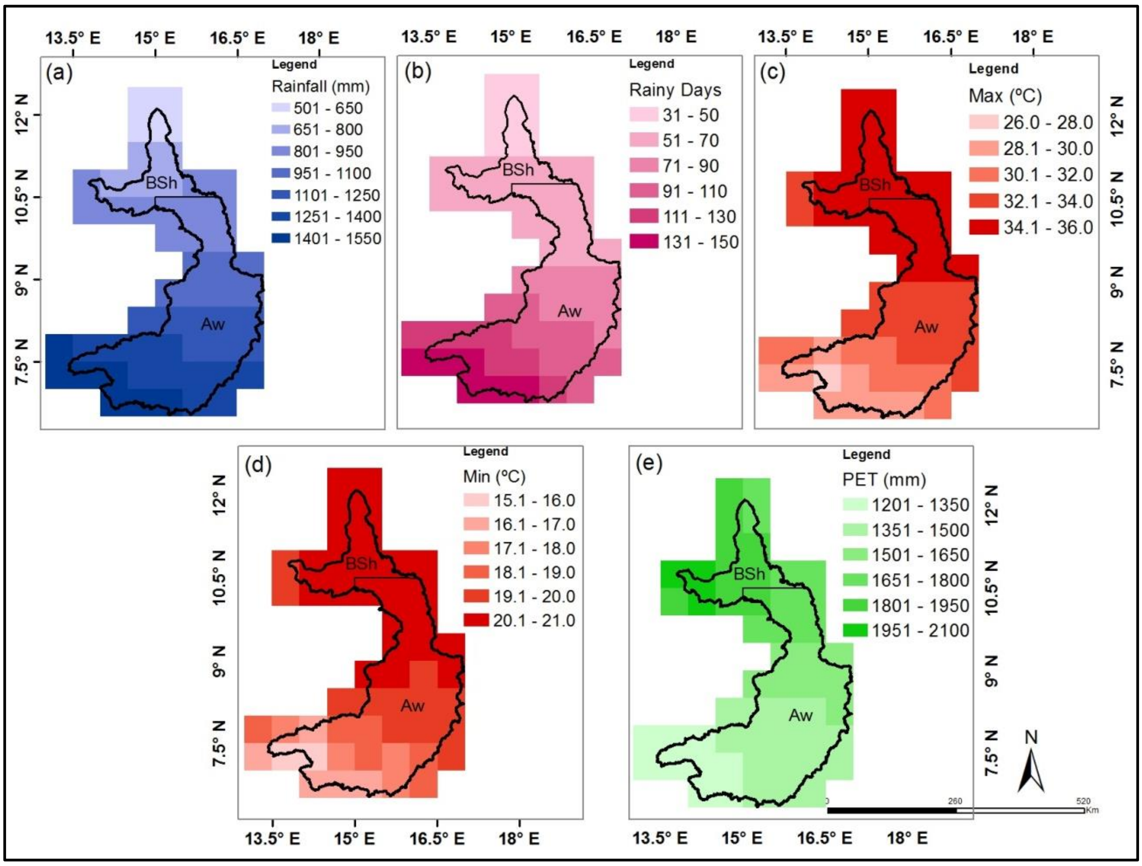

Fig. 2. Spatial distribution of annual climatic parameters over the Logone basin, including (a) Rainfall, (b) Number of Rainy Days, (c) Maximum Temperature, (d) Minimum Temperature and (e) PET

4.1 Changes in Annual Climatic Parameters

4.1.1 Temporal Variability Summarized by Climate Zones

The linear trend line equations and t-statistics for annual rainfall of both climatic zones for the entire duration are given in Fig. 3a. Annual rainfall decreased in both climatic zones over the entire duration (Fig. 3a). The regression equations for number of rainy days are y = -0.0195x + 96.697 (t=-1.427) and y = -0.0135x + 48.169 (t=-1.241) for Aw and BSh climatic zones, respectively. A non-significant decreasing trend was observed in annual rainfall and number of rainy days of both climatic zones of the basin from 1901-2013 (Fig. 3a &Table S2).

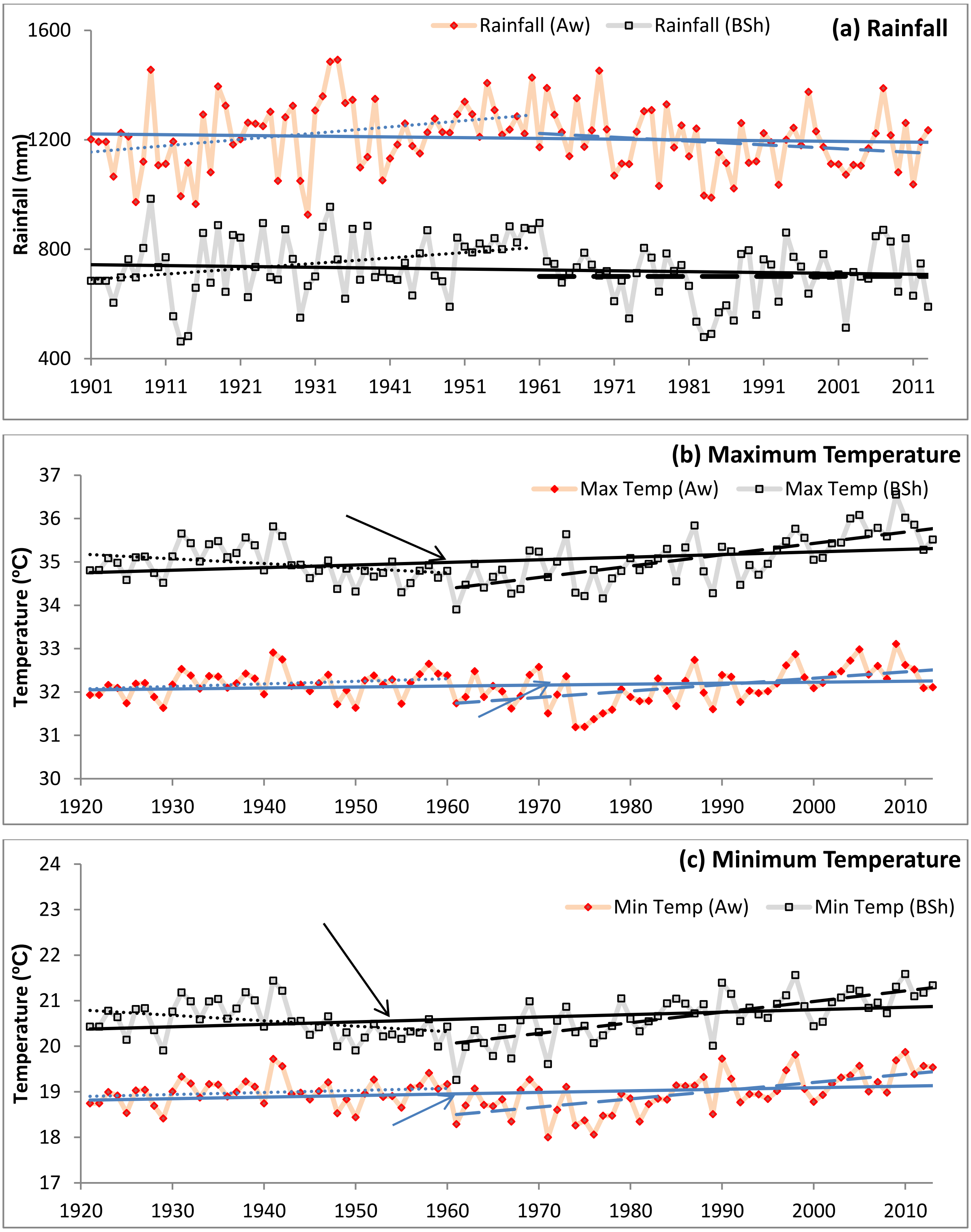

Fig. 3. Annual time series with a linear regression trend line (a) Rainfall, (b) Maximum and (c) Minimum Temperatures *(Note: Solid, dotted and dashed lines represent linear trend lines during the entire, pre-1960 and post-1960 durations,respectively. Blue and black colour lines indicate the trend lines for Aw and BSh zones, respectively.)*

The time-series of average annual maximum and minimum temperatures in the two climatic zones are shown in Fig. 3b and 3c with linear regression trend lines. Positive slopes of trend lines for the entire duration (1921-2013) indicate warming in both zones. Furthermore, negative slopes of linear regression trend lines during pre-1960 for maximum and minimum temperatures in the BSh zone suggest cooling (Table S2), contrasting with trends in Aw during this period (Table S2). The steeper, positive slopes for all the temperature series during post-1960 in both zones suggest an accelerated warming effect. The regression equation and trend line significance are given in Fig. 3b and 3c. Significant increasing trends were observed in maximum and minimum temperatures of the both climatic zones of the basin, except for the maximum temperature of the Aw zone during pre-1960. For BSh, maximum temperature increases faster than minimum temperature whereas minimum temperature increases faster than the maximum temperature for Aw zone (Figure 3b and 3c). The regression equation of climatic parameters for Aw and BSh zones for all duration is given in supporting material (Table S2).

4.1.2 Spatio-temporal Variability Summarized Grid by Grid

The trend analyses for rainfall, temperatures (maximum and minimum) and PET for all three durations and two climatic zones are shown in Fig. 4. The Z-statistics values of MK/MMK test are given in the supporting material for entire duration (Table S3).

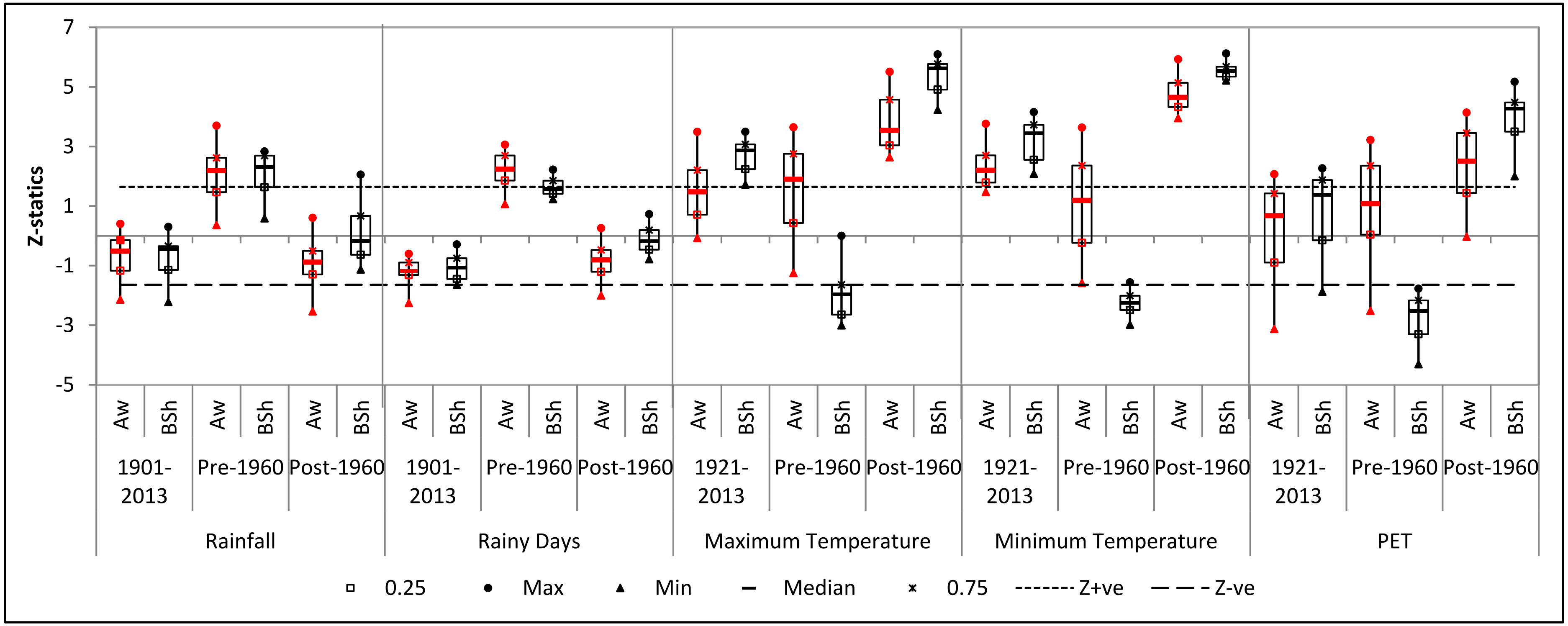

Fig. 4. Z-statistics of annual climatic parameters for Aw and BSh climatic zones of the basin for three durations. (Note: Positive and negative Z-statistic values indicate increasing and decreasing trends, respectively. Z-statistic values outside the range of ±1.645 i.e. dashed lines represent significant trends. Red and black color boxes used for Aw and BSh zones, respectively.)

Annual rainfall and the number of rainy days showed an overall decreasing trend over the entire duration of 1901-2013 but these trends were not statistically significant. Conversely, annual rainfall and rainy days significantly increased during pre-1960 and there was a non-significant decreasing trend for post-1960. The trends for annual rainfall and number of rainy days did not differ across the Aw and BSh spatial zones.

The annual maximum and minimum temperatures from 1921-2013 show increasing trends in most of the grids of each climatic zone. In general, trends in the BSh zone are more clustered relative to those of the Aw zone (Fig. 4) The maximum temperatures in some Aw grid cells and for some BSh grid cells have decreasing trends during pre-1960. However, during post-1960, all grid cells of both climatic zones show significant increasing trends for maximum temperatures. Minimum temperatures showed similar tendencies during the two partial durations, with decreasing trends in pre-1960 and significant increasing trends in the post-1960 period. The trend reversal of temperatures is more prominent in the BSh zone than in Aw. The annual PET increased over the basin from 1921-2013 (Fig. 4). During pre-1960 period, most of the grid cells had non-significant increasing trends of PET in the Aw climatic zone, but significant decreasing trends of PET in the BSh zones. However, significant increasing trends have been observed in PET of both climatic zones during post-1960.

The spatial pattern of trends in annual climatic parameters of both climatic zones of the basin is shown in Fig. 5. When considering the entire duration (1901-2013), most grids in both climatic zones showed negative changes ranging from -0.1 to -12.4% for annual rainfall (Fig. 5-i a,). From pre-1960, all grids in the basin showed positive changes in annual rainfall with magnitudes ranging from 2.2 to 28.2% (Fig. 5-ii b). The largest relative changes (>20%) occurred in the far north; this represents a major change in direct rainfall on the floodplain. Conversely, during post-1960, nearly all grid cells showed a reduction in annual rainfall, with magnitudes as low as -14.3% (equivalent to 122.7 mm). The largest relative changes were again in the north, and mostly positive, in part because of the lower annual average base rainfall there. The most extreme drought conditions occurred during 1968-1997 with some recovery in the early 21st century on the floodplain (BSh zone rainfall). The spatial variability of the average number of rainy days over the basin (given in supporting material; Figure S1-i (a-c)) resembles that for the average annual rainfall. In watershed, on average the rainfall intensity got increased across the grids in post-1960 as compared to pre-1960 (See in supporting material; Figure S2). However, the rainfall intensity got decreased across the grids in the BSh zone in recent duration (See in supporting material; Figure S3).

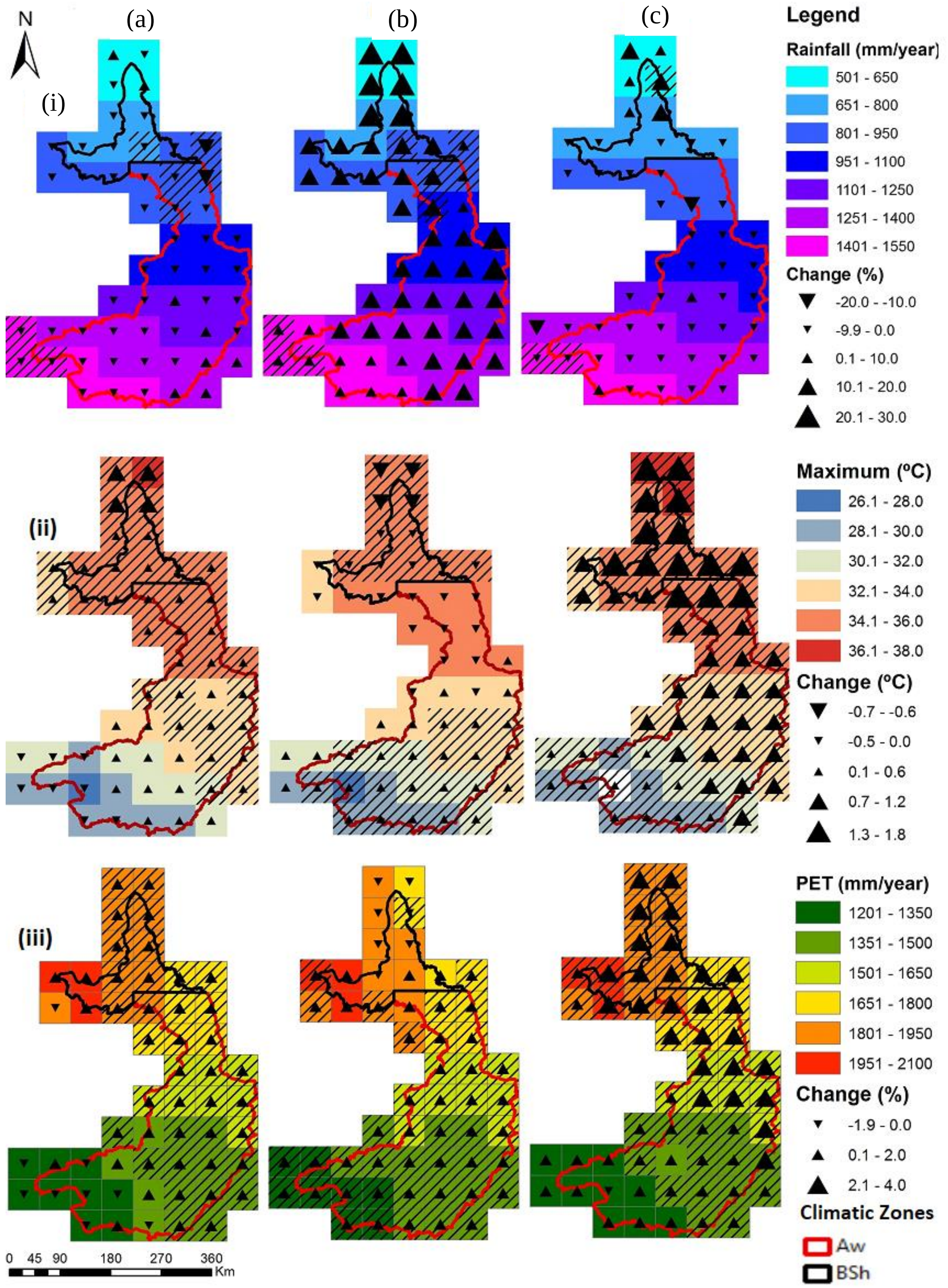

Fig. 5. Variability in annual (i) Rainfall (first row), (ii) Maximum Temperature (second row) and (iii) PET (third row) over the basin during (a) 1901/1921-2013, (b) pre-1960 and (c) post-1960. Shaded grids indicate significant change

The spatial pattern of trends in annual maximum temperature is shown in Fig. 5-ii (a-c). For 1921-2013, the largest trends are observed in the BSh zone, while lesser warming and/or cooling occurred throughout the Aw zone. The BSh zone exhibited large temperature changes: from pre-1960 there was a -0.1 to -0.7°C change in maximum temperature, and during post-1960 there was +1 to +1.8°C change in maximum temperature (Table 1).

Significant spatial variability in temperature exists in the Aw zone. In northern grid cells in the Aw zone, from pre-1960, there were -0.2 to +0.6°C changes in maximum temperatures, and +0.5 to +1.3°C changes in maximum temperature post-1960 (Table 1). Changes are generally smaller and less likely to be significant in the Logone headwaters, to the south. A similar spatial pattern was observed in annual minimum temperature (not shown, provided as supporting material; Figure S1-ii).

The greatest change (+3 to +4%) in PET is observed in grids of BSh zone during post-1960 (Fig. 5-iii c). The percent of change of annual PET has increased from upstream (Aw) to downstream (BSh) of the basin.

4.1.3 Change Magnitudes of Annual Climatic Parameters by Climatic zones

Table 1 summarizes the magnitudes of changes in climatic parameters across the two climatic zones for the entire and two partial durations. The magnitudes are summarized in terms of spatial average based on all grid cells within each climatic zone, the significance of the mean change, and the range (minimum and maximum evaluated across grid cells).

Table 1: Magnitude of climatic parameter change. Values of the spatial minimum, maximum, and mean (in parentheses) are shown, and * indicates a significant change (in either direction) based on MK/MMK test at alpha = 0.1.

Zone	Parameter/ Duration	Rainfall (mm)	Rainy Days (Days)	Max Temp (°C)	Min Temp (°C)	PET (mm)
Aw	**1901/1921-2013**	-112 to +21 (-33)	-5 to -1 (-2)	0.0 to +0.5 (+0.2)	+0.2 to +0.6 (+0.3)*	-16 to +15 (+2)
	Pre-1960	+32 to +246 (+138)*	+3 to +9 (+5)*	-0.2 to +0.6 (+0.3)*	-0.3 to +0.6 (+0.2)*	-9 to +8 (+1)
	Post-1960	-164 to +41 (-64)	-6 to +1 (-2)	+0.5 to +1.3 (+0.8)*	+0.8 to +1.3 (+1.0)	0 to +50 (+24)*
BSh	**1901/1921-2013**	-103 to +10 (-32)	-2 to 0 (-2)	+0.3 to +0.8 (+0.5)*	+0.3 to +0.7 (+0.5)*	-19 to +29 (+10)
	Pre-1960	+27 to +162 (+126)*	+2 to +5 (+3)*	-0.7 to -0.1 (-0.4)*	-0.8 to -0.3 (-0.5)*	-10 to +15 (+5)
	Post-1960	-64 to +111 (+0.4)	-2 to +2 (0)	+1.0 to +1.8 (+1.4)*	+1.1 to +1.3 (+1.2)*	+26 to +72 (+53)*

The estimated change magnitudes suggest a reduction of annual rainfall by about 33 mm across both climatic zones over the entire duration (1901-2013). Although the average magnitude of reduction is statistically non-significant (t-value=-1.444), the rainfall changes at individual grid cells range from -112 to +21 mm across the Aw zone. Analysis based on the initial period (1901-1960), suggests a significant (t-value=2.541) increase in rainfall with average change of about +138 mm, and a range of +32 to +246 mm across Aw. These trends seem to have reversed in the Aw zone during 1961-2013 with an average change of about -64 mm and a range of -164 to -41 mm. Similarly, rainfall increased in the BSh zone in the earlier period by an average of 126 mm; this change is statistically significant, and relatively large (nearly 20%) compared to average annual rainfall of 740 mm, in this zone.

The annual maximum and minimum temperatures showed increasing trends during both the durations with an increase of about 0.8°C and 1.0°C during 1961-2013 compared to 0.3°C and 0.2°C during 1901-61 in Aw climatic zone. The annual maximum and minimum temperature showed decreasing trend (-0.4°C and -0.5°C) during 1921-1960, which gets reversed as increasing trend (1.4°C and 1.2°C) during 1961-2013 in BSh climatic zone.

4.2 Changes in Seasonal Climatic Parameters

4.2.1 Rainy Season

Trend analyses for all climatic parameters evaluated for the rainy season are shown in Table 2, where the number of grid cells showing increasing or decreasing trend is presented, broken out by statistical significance. Changes in rainy season rainfall across grid cells over three periods showed mixed levels of significant change. Over the entire period, for the Aw zone, 16 out of 39 grid cells show an increase in rainfall, but a decrease in rainy days, although none of these changes are statistically significant. However, such changes are suggestive that rainfall intensity may be increasing on average, leading to more rainfall in fewer events. Approximately 58% of the grid cells located in the Aw zone showed decreasing rainy season rainfall with significant decrease in 3 grid cells. Rainfall during rainy season increased in only 2 out of 15 grids cells in the BSh zone with remaining most of the cells showing the non-significant decreasing change over the entire period.

Table 2: Number of grids showing increasing and decreasing trends in the climatic parameters for Aw and BSh climatic zones of the basin during the rainy season

Climatic Parameters	Zones / Trend	Aw 1901/21-2013	Aw pre-1960	Aw Post-1960	BSh 1901/21-2013	BSh pre-1960	BSh Post-1960
Rainfall	Increasing	0|16	31|39	0|4	0|2	12|15	1|6
	Decreasing	3|23	0|0	3|35	1|13	0|0	0|9
#Rainy days	Increasing	0|0	33|39	0|3	0|0	8|15	0|4
	Decreasing	1|39	0|0	2|36	0|15	0|0	0|11
Maximum temperature	Increasing	28|38	14|26	39|39	15|15	0|0	15|15
	Decreasing	0|1	7|13	0|0	0|0	15|15	0|0
Minimum temperature	Increasing	39|39	15|27	39|0	15|0	0|0	15|15
	Decreasing	0|0	2|12	0|0	0|0	14|15	0|0
PET	Increasing	11|27	13|27	26|36	7|12	0|0	14|15
	Decreasing	6|12	6|12	0|3	1|3	15|15	0|0

Note: The denominator represents the total number of grids with increasing/decreasing trends and the numerator represent the number of grids showing statistically significant trends at 10% significance level (MK/MMK test).

A significant increasing trend was observed in both maximum and minimum temperatures for most of the grid cells during the entire period, as well as for the data since 1960, for both the climatic zones. Most of the grid cells in Aw and BSh climatic zones showed increasing maximum and minimum temperatures for the entire period except, 1 grid cell showed non-significnt decreasing trends during the rainy season. The maximum and minimum rainy season's temperatures for both climatic zones behave differently during the pre-1960. The significant increasing maximum temperature trends were observed for most of the grids of the Aw 14 zone and whereas significant decreasing trends were observed for all 15 grid cells for BSh climatic zones during pre-1960. Increasing trends were observed in seasonal PET for both climatic zones during all durations, except for the BSh zone from pre-1960.

The magnitude of changes in climatic parameters across the two climatic zones for the entire and two partial durations for rainy season are given in Table S4 and Figure S4. It indicates that on average the rainfall is decreased by -4.7% in Aw zone whereas increased by 1.4% in BSh zones during the recent years. Both maximum and minimum temperatures are increased by 0.8°C in Aw zone. Also, the temperatures of the BSh zone are increased by 1.4°C during the recent years. It indicates that the basin is getting warmer and facing the water scarcity problems in recent years.

4.2.2 Dry Season

Results from the trend analyses for all climatic parameters evaluated for the dry season are shown in Table 3. A significant decreasing trend was observed in dry season rainfall over the entire study period for both the climatic zones. A non-significant decreasing trend was observed in dry season rainfall for the Aw climatic zone during both partial series. Significant decreasing and increasing trends were observed in rainfall of dry season during the pre-1960 and post-1960 for the BSh climatic zone, respectively.

The number of rainy days during the dry season significantly decreased over the period from 1901-2013. Non-significant and significant decreasing trends were observed in the number of rainy days of dry season during the pre-1960 for Aw and BSh climatic zones respectively. In contrast, the non-significant increasing trends were observed in the number of dry season rainy days for the BSh zone during the recent duration.

Table 3: Number of grids showing increasing/ decreasing trends in the climatic parameters for Aw and BSh climatic zones of the basin during the dry season

Climatic Parameter	**Zones**	**Aw**			**BSh**		
	Trend	**1901/21-2013**	**Pre-1960**	**Post-1960**	**1901/21-2013**	**Pre-1960**	**Post-1960**
Rainfall	Increasing	0/0	0/7	1/19	0/0	0/0	8/14
	Decreasing	36/39	5/32	1/20	12/15	9/15	0/1
# Rainy Days	Increasing	0/3	3/14	0/12	0/1	2/3	1/15
	Decreasing	33/36	4/25	0/27	9/14	9/12	0/0
Maximum Temperature	Increasing	1/15	27/39	39/39	0/13	3/9	15/15
	Decreasing	0/24	0/0	0/0	0/2	0/6	0/0
Minimum Temperature	Increasing	1/39	13/31	39/0	1/15	0/0	15/15
	Decreasing	0/0	0/8	0/0	0/0	5/15	0/0
PET	Increasing	0/20	16/34	16/39	0/9	0/0	15/15
	Decreasing	1/19	0/5	0/0	2/6	5/15	0/0

Note: Value in denominator represents the total number of grids with increasing/decreasing trends. Value in numerator represents the number of grids showing statistically significant trends at 10% significance level (MK/MMK test).

A non-significant decreasing trend was observed for dry season maximum temperature over the entire duration. However, a significant increasing trend was observed during recent years. A non-significant decreasing trend was observed in maximum dry season temperature during pre-1960 for the BSh zone. A non-significant increasing trend was observed in minimum temperature of dry season for both the climatic zones during the entire duration, whereas both climatic zones show a significant increasing trend in minimum temperature of the dry season during the recent duration. Increasing trends were observed in seasonal PET for the grid cells of both climatic zones during all durations, except for the BSh zone from pre-1960. The magnitude of changes in climatic parameters across the two climatic zones for the entire and two partial durations during rainy season are given in Table S4. It indicates that on average dry season maximum and minimum temperatures are increased by 0.8°C and 1.3°C for Aw climatic zone whereas by 1.3°C for BSh zones, indicating the basin is getting more dry/hot during the dry season during the recent years.

5. Discussion

Impacts of climatic changes on floodplain hydrologic processes

In the Logone floodplain and other African floodplains, seasonal flooding is important as a source of life, supporting agriculture, fishery and pastoralism (Loth 2004). Too much or inadequate flooding negatively impact the lives and livelihoods of populations in floodplains. Changes in the BSh zone rainfall and PET directly impact the water balance of the floodplain, with both terms playing a major role in driving floodplain mass balance (Delclaux et al. 2010; Fernandez et al. 2016). In contrast, climatic variations in the Aw zone rainfall and PET are expected to change the flows and flow patterns of the Logone River, driving variations in overbank flooding, which is the primary control on floodplain inundation. This will lead to changes in the inundation extent of the floodplains that would eventually affect fish migration, geomorphology, as well as the vegetation distribution.

Our results highlight the importance of rainfall temporal variability on the floodplain. Detected changes in rainfall during the study period may determine fluctuations in the flooding patters. Although rainy season rainfall does not show a significant change, the increase in the number of rainy days, the rainfall decrease in the dry season together with less rainy days, suggest a more concentrated period of rain, perhaps changing flooding seasonality and intensity. This may be leading to more uncertainty in the timing of activities of pastoralism and fishing or introduce additional pressures to operating socio-ecological feedbacks. For example, Laborde et al. (2016) report an increasing trend in fishing canals, built to maximize capture and profit, and demonstrate that they impact the local hydrology. These fishing canals are most utilized during the flooding recession; more concentrated rainfall may make more difficult this activity as the flooding recession may become less predictable.

Analysing more specifically each climatic zone, the floodplain which falls in the BSh zone, the long-term (pre-1960) increase in rainfall of approximately 20% would be expected to lead to changes in floodplain inundation, and floodplain industries. This impact of rainfall variations on livelihoods is in agreement with other semi-arid regions (The World Bank 2009). Understanding the historical variations of rainfall in the BSh zone over the floodplain is important in the design of experiments for exploring the role of future climate variations on floodplain inundation.

The impact of rainfall variations on overbank flow can be assessed by relating rainfall in the Aw zone to streamflow at the Bongor gauging station (see Fig. 1). Rainfall and streamflow from 1954-1995 are plotted in Fig. 6. There is a strong correlation between the two quantities, with R^2=0.64. This time period was limited by the availability of runoff data. The trend line between rainfall and runoff has a slope of approximately 0.4 (Fig. 6b); it also reinforces the finding of MacDonald (1993) that small changes in rainfall lead to large changes in streamflow. For example, a decrease in rainfall from 1200 to 1000 mm/year is a change of just 17% in terms of rainfall, but leads to a change from 262 to 177 mm/year of streamflow, a change of 32% in terms of streamflow. Given that our analysis indicates that multi-decadal changes of over 100 mm/year have occurred for pre-1960, these dynamics are of utmost importance in understanding possible future changes in floodplain inundation. Note that there is a significant decreasing trend in both rainfall and runoff from 1954-1995. Comparison with Fig. 5 (i-c) indicates that rainfall increased again from 1995-2013.

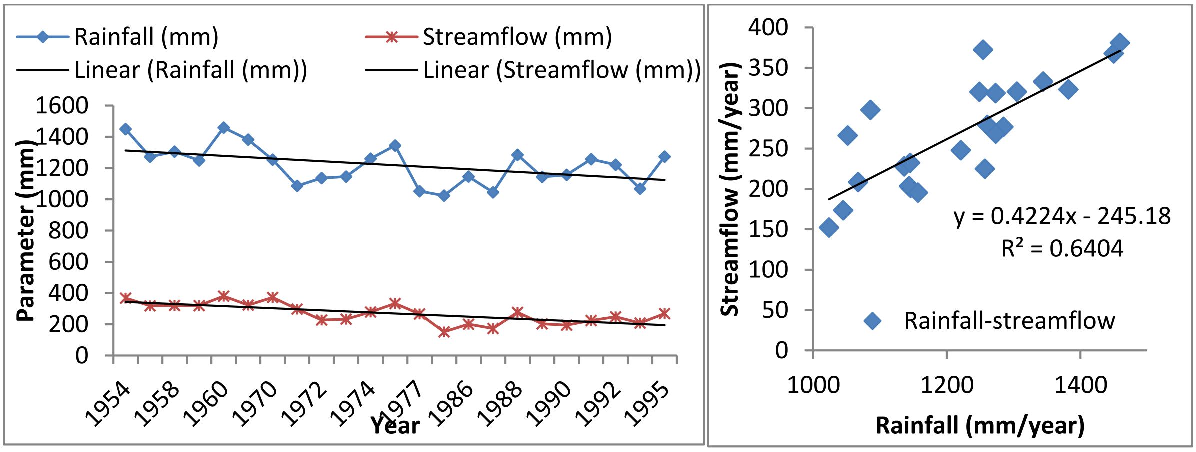

Fig. 6. (a) Annual Rainfall of contributing grids in Aw zone and annual streamflow trend line and (b) Relationship between rainfall of Aw zone and streamflow at Bongor

Evapotranspiration plays a major role in the floodplain water balance in the BSh zone (Delclaux et al. 2010), as well as driving the runoff processes controlling Logone streamflow in the Aw zone. Indeed, with annual rainfall and PET of approximately 1200 and 1600 mm/year, respectively, runoff in the Logone watershed is slightly water limited; changes in PET would be expected to impact streamflow. The 53 mm PET increase in the BSh zone doubles that observed in the Aw zone. Given that actual ET fluxes from the floodplain itself can be greater than two meters based on pan evaporation measurements (Delclaux et al. 2010), past changes will not likely impact the overall water balance of the floodplain directly. Similarly, the 24 mm increase in PET in the Aw zone will not likely impact the Logone streamflow enough to cause significant changes in inundation. As a measure of evapotranspiration independent of surface conditions, PET will differ from actual ET (Shelton, 2009), but increased PET demands and lack of soil moisture during critical growth stages of crops may have considerable impacts on productivity in the region. The relationship between PET and actual ET also depends on crop type, and antecedent soil moisture conditions (Allen et al. 1998). Furthermore, increased PET demands and lack of soil moisture during critical growth stages of crops may have considerable impacts on crop productivity in the region.

The observed temperature changes will not directly impact inundation processes, but may disturb fishery operation, agriculture, and other social and ecological systems on the floodplain due to its relationship with atmosphere moisture capacity and hence rainfall intensity (Westra et al. 2014). Prior studies indicate a warming trend over the African continent since the 1960s, but these changes are not always uniform spatially (Boko et al. 2007; Rubel and Kottek 2010; Nash et al. 2016). McSweeney et al. (2010) reported that the number of very hot days per year doubled since the 1960s in West Africa. Our analysis shows significant increases in annual maximum and minimum temperatures with an increase of about 0.8°C and 1.0°C during post-1960 compared to 0.3°C and 0.2°C during pre-1960 in Aw climatic zone respectively. The annual maximum and minimum temperatures showed decreasing trend (maximum = -0.4°C and minimum = -0.5°C) during pre-1960 with an increasing trend (maximum = 1.4°C and minimum = 1.2°C) during post-1960 in the BSh climatic zone. The rate of increased minimum temperature is higher than the maximum temperature in both climatic zones. A perceived change in temperatures and rainfall patterns causes reduction in crop production or causes a change in soil moisture conditions (Sonneveld et al. 2011). We found significant spatial and temporal variation in climatic parameters across the Logone River basin associated with flooding on the downstream Logone floodplain. The changes in rainfall and PET will impact the spatial patterns of water availability, which will influence the social-ecological systems in the Logone Floodplain. Changes in rainfall may affect the streamflow of the river and its flooding patterns, which shape the vegetation and fish populations in the floodplain, which directly affect the livelihoods of herders and fishers respectively.

6. Conclusions

The impact of long-term climatic variations were examined using the CRU dataset in this study considering its possible impacts on flooding. This dataset is the best available database because it is a trade-off between long-term continuity and spatial resolution, which makes it a better choice relative to in-situ observations and reanalyses. Specifically, rainfall across the Aw (upstream south, mainly in the watershed region) region is a key driver of flooding. Rainfall significantly increased in the pre-1960 period, but decreased post-1960, compared to the long-term basin average. Temperatures and PET increased over the entire 1901/1921-2013 period, with the largest increase post-1960. However, the magnitude of PET changes over this period are not enough to significantly impact either the hydrologic balance on the floodplain or downstream Logone discharge.

The increasing trends in minimum, as well as maximum temperatures suggest a shift in magnitude as well as the spatial extent of the temperature regimes, causing a northward shift in the boundaries of the climatic zones. This shift in temperature regimes may have serious implications for agriculture by reducing rainfed practices in the basin. Moreover, the hydroclimatic trends over the floodplain itself (i.e. over the BSh zone) are distinct from those over the large Logone River watershed (the Aw zone). Thus, projections of climate change impacts on future flooding in the floodplain need to consider the cumulative influence of these two climatically different regions. Further studies can be done using different datasets such as Coordinated Regional Climate Downscaling Experiment (CORDEX) which have a finer temporal resolution than CRU. Also, this dataset offers both historical and projected climate. It is important to quantify the impact of future climatic changes on the hydrological process and floodplain dynamics of the region using Global Climate Models and hydrological modeling. Therefore, it is useful to analyse the spatio-temporal changes of future climate of the Logone basin which is helpful in the planning of adaptation and mitigation policies to cope with anticipated consequences of future climate variability on flooding pattern.

Acknowledgements

The study is financially supported by the NSF Dynamics of Coupled Natural and Human Systems (CNH) program to Modeling Regime Shifts in the Logone floodplain (MORSL)

(BCS-1211986). The authors would like to thank Vinayak Shedekar (OSU, Columbus, USA) and Michael Brooker (OSU, Columbus, USA) for critical feedback on the paper and proof-reading it. The authors also would like to thank Arun Kumar Taxak (IIT Roorkee, India) and Steven Chouto (University of Maroua, Cameroon) for their helpful discussion during the data analysis.

References

Abtew, W., Obeysekera, J. and Iricanin, N., 2011. Pan evaporation and potential evapotranspiration trends in South Florida. *Hydrol Process* 25: 958-969.

Acreman, M.C. and Hollis, E.G., 1996 Water management and wetlands in sub-Saharan Africa. IUCN, Gland.

Allen, R.G., Pereira L.S., Raes D., ans Smith M., 1998. Crop evapotranspiration – Guidelines for computing crop water requirements – FAO Irrigation and Drainage Paper 56.

Anderson, R.L., 1942. Distribution of the Serial Correlation Coefficient. *Ann. Math. Statist*. 13 (1): 1-13. doi:10.1214/aoms/1177731638.

Assan, J., Caminade, C. and Obeng, F., 2009. Environmental variability and vulnerable livelihoods: minimizing risks and optimizing opportunities for poverty alleviation. *J Int Dev* 21(3):403-418.

Basistha, A., Arya, D.S. and Goel, N.K., 2009. Analysis of Historical rainfall change in Indian Himalayas. *International Journal of Climatology*, 29:555-572.

Bastola, S.; Francois, D. Temporal extension of meteorological records for hydrological modelling of Lake Chad Basin (Africa) using satellite rainfall data and reanalysis datasets. *Meterological Application*, 19:54-70.

Boko, M., Niang, I., Nyong, A., Vogel, C., Githeko, A., Medany, M., Osman-Elasha, B., Tabo, R. and Yanda, P., 2007. Africa Climate Change 2007: Impacts, Adaptation and Vulnerability. Contribution of Working Group II to the Fourth Assessment Report of the Intergovernmental Panel on Climate Change, Parry ML, Canziani OF, Palutikof JP, van der Linden PJ, Hanson CE, Eds., Cambridge University Press, Cambridge UK, 433-467.

Christensen, J.H., Hewitson, B., Busuioc, A., Chen, A., Gao, X., Held, I., Jones, R., Koli, R.K., Kwon, W.T., Laprise, R., Rueda, V.M., Mearns, L., Menéndez, C.G., Räisänen, J., Rinke, A., Sarr, A. and Whetton, P., 2007. Regional climate projections. Climate Change 2007: The Physical Science Basis. Contribution of Working Group I to the Fourth Assessment Report of the Intergovernmental Panel on Climate Change.

Solomon S, Qin D, Manning M, Chen, Marquis M, Averyt KB, Tignor M, Miller HL, Eds. Cambridge University Press, Cambridge, 847-940.

Cook, K.H. and Vizy, E.K., 2015. The Congo Basin Walker circulation: dynamics and connections to precipitation. *Climate Dynamics*. pp 1-21.

Cunderlik, M.J. and Burn, D.H., 2004. Linkages between Regional Trends in Monthly Maximum Flows and Selected Climatic Variables. *ASCE Journal of Hydrologic Engineering*, 9(4): 246-256.

Delclaux, F., Seignobos, C., Liénou, G. and Genthon, P., 2010. Water and people in the Yaéré floodplain (North Cameroon). In: Álvarez MA (ed.), Floodplains: physical geography, ecology and societal interactions. Hauppauge, New York: Nova Publishers. pp 1-27.

Fernández, A., Najafi, N.R., Durand, M., Mark, B.G., Moritz, M., Neal, J., Shastry, A., Laborde, S., Phang, S.C., Hamilton, I.M. and Xiao, N., 2016. Testing the skill of numerical hydraulic modeling to simulate spatiotemporal flooding patterns in the Logone floodplain, Cameroon. *Journal of Hydrology*, 539:265-280.

Geiger, R., 1954. Landolt-Börnstein – Zahlenwerte und Funktionen aus Physik, Chemie, Astronomie, Geophysikund Technik, alte Serie Vol. 3, Ch. Klassifikation der Kli-mate nach W. Köppen. – *Springer, Berlin*. 603-607.

Goyal, R.K., 2004. Sensitivity of evapotranspiration to global warming: a case study of arid zone of Rajasthan (India). *Agric Water Manage* 69:1-11.

Haan, C.T., 1995. Statistical Methods in Hydrology, Iowa State University Press, 1995.

Harris, I., Jones, P.D., Osborna, T.J. and Listera, D.H., 2014. Updated high-resolution grids of monthly climatic observations – the CRU TS3.10 Dataset. *Int. J. Climatol*. 34: 623-642. DOI: 10.1002/joc.3711.

Hulme, M., Mitchell, J.F.B., Ingram, W., Johns, T.C., Lowe, J.A., New, M.G. and Viner, D., 1999. Climate change scenarios for global impacts studies. *Global Environmental Change*, (9): S3-S19.

Kendall, M.G., 1955. Rank Correlation Methods. Griffin, London.

Kittel, T.G.F., Rosenbloom, N.A., Painter, T.H., Schimel, D.S., VEMAP Modeling Participants, 1995. The VEMAP integrated database for modeling United States ecosystem/vegetation sensitivity to climate change. *Journal of Biogeography*, (22): 857-862.

Köppen, W., 1900. Versuch einer Klassifikation der Kli-mate, vorzugsweise nach ihren Beziehungen zur Pflanzen-welt. – *Geogr. Zeitschr*. 6, 593–611: 657-679.

Kottek, M., Grieser, J., Beck, C., Rudolf, B. and Rubel, F., 2006. World map of the Köppen-Geiger climate classification updated. *Meteorol. Z.* 15: 259-263.

Laborde, S., Fernandez, A., Phang, S.C., Hamilton, I.M., Henry, N., Jung, H.C., Mahamat, A., Ahmadou, M., Labara, B., Kari, S., Durand, M., Mark, B., Xiao, N., Ziebe, R. and Moritz, M., 2016. Social-ecological feedbacks lead to unsustainable lock-in in an inland fishery. *Global Environmental Change*, 41 (November 2016):13-25.

Leblanc, M.; Lemoalle, J.; Bader, J.C.; Tweed, S.; Mofor, L. 2011. Thermal remote sensing of water under flooded vegetation: New observations of inundation patterns for the "Small" Lake Chad. *J. Hydrol*. 404: 87–98.

Loth, P., (ed.). 2004. The return of the water. Gland: IUCN.

Loth, P., Moritz, M., Kouokam, R., Scholte, P., Kari, S. 2004. The People of the Floodplain. Chapter 7 in: The return of the water Restoring the Waza Logone floodplain in Cameroon. Restoring the Waza Logone. Loth, P. (Ed)., 53-67.

MacDonald, M., 1993. Mathematic Model of the Hydrological Behaviour of Lake Chad and Its Feeder Rivers. Mott MacDonald, Cambridge.

Mahlstein, I., Knutti, R., Solomon, S. and Portmann, R., 2011. Early onset of significant local warming in low latitude countries. *Environ. Res. Lett*., 6, 034009, doi:10.1088/1748-9326/6/3/034009.

Mahmood R, Jia S. 2018. Analysis of causes of decreasing inflow to the Lake Chad due to climate variability and human activities. Hydrol. Earth Syst. Sci. Discuss.:1–42. doi: 10.5194/hess-2018-139.

Mahmood, R., Jia, S. and Zhu, W. 2019. Analysis of climate variability, trends, and prediction in the most active parts of the Lake Chad basin, Africa. Scientific reports., 9(1): 6317.

Malhi, Y. and Wright, J., 2004. Spatial patterns and recent trends in the climate of tropical rainforest regions. *Philos. T. Roy. Soc. B*, 359: 311-329.

Mann, H.B., 1945. Non-Parametric Tests against Trend. *Econometrica*, 13:245-259.

McSweeney, C., New, M., Lizcano, G. and Lu, X., 2010. The UNDP Climate Change Country Profiles Improving the Accessibility of Observed and Projected Climate Information for Studies of Climate Change in Developing Countries. *Bulletin of the American Meteorological Society*, 91: 157-166.

Milly, P.C.D., Dunne, K.A. and Vecchia, A.V., 2005. Global pattern of trends in streamflow and water availability in a changing climate. *Nature* 438: 347-350.

Mitchell, S.A., 2013. The status of wetlands, threats and the predicted effect of global climate change: the situation in Sub-Saharan Africa. *Aquat Sci*. 75:95-112.

Moritz, M., Laborde, S., Phang, S.C., Ahmadou, M., Durand, M., Fernandez, A., Hamilton, I.M., Kari, S., Mark, B., Scholte, P., Xiao, N. and Ziebe, R., 2016. Studying the Logone floodplain, Cameroon, as a coupled human and natural system. *African Journal of Aquatic Science*, 41(1): 99-108, DOI: 10.2989/16085914.2016.1143799.

Nash, D.J., De Cort, G., Chase, B.M., Verschuren, D., Nicholson, S.E., Shanahan, T.M., Asrat, A., Lézine, A.M. and Grab, S.W., 2016. African hydroclimatic variability during the last 2000 years. *Quaternary Science Reviews*, 154: 1-22.

New, M., Hewitson, B., Stephenson, D.B., Tsiga, A., Kruger, A., Manhique, A., Gomez, B., Coelho, C.A.S. and Co-authors., 2006. Evidence of trends in daily climate extremes over southern and west Africa. *J. Geophys. Res.–Atmos*., 111, D14102, doi:10.1029/2005JD006289.

Nicholson, S.E., Some, B. and Kone, B., 2000. An analysis of recent rainfall conditions in West Africa, including the rainy season of the 1997 El Niño and the 1998 La Niña years. *J. Climate*, 13: 2628-2640.

Nicholson, S.E. and Yin, X.G., 2001. Rainfall conditions in equatorial East Africa during the nineteenth century as inferred from the record of Lake Victoria. *Clim. Change*, 48: 387-398.

Rubel, F. and Kottek, M., 2010. Observed and projected climate shifts 1901-2100 depicted by world maps of the Köppen-Geiger climate classification. *Meteorol. Z.*, 19, 135-141. DOI: 10.1127/0941-2948/2010/0430.

Savo, V., Lepofsky, D., Benner, J.P., Kohfeld, K.E., Bailey, J. and Lertzman, K., 2016. Observations of climate change among subsistence-oriented communities around the world. *Nature Climate Change* 4: 462-473. DOI: 10.1038/NCLIMATE2958.

Scholte, P., 2005. Floodplain rehabilitation and the future of conservation and development: adaptive management of success in Waza-Logone, Cameroon. Leiden: Leiden University Press.

Sen, P.K., 1968. Estimates of the regression coefficient based on Kendall's tau. *Journal of American Statistical Association*, 63:1379-1389.

Shadmani, M., Marofi, S. and Roknian, M., 2011. Trend Analysis in Reference Evapotranspiration using Mann-Kendall and Spearman's Rho tests in Arid Regions of Iran. *Water resource management* 26: 211-224. DOI 10.1007/s11269-011-9913z.

Spinoni, J., Naumann, G. and Vogt, J.V., 2017. Pan-European seasonal trends and recent changes of drought frequency and severity. *Global and Planetary Change* 148:113-130.

Sonneveld BGJS, Keyzer MA, Adegbola P, Pande S., 2011. The Impact of Climate Change on Crop Production in West Africa: An Assessment for the Oueme River Basin in Benin. Water Resources Management. 26(2): 553–79. doi: 10.1007/s11269-011-9931-x.

The World Bank., 2009. World Day to Combat Desertification 2009. http://www.worldbank.org/en/news/feature/2009/06/16/world-day-to-combat-desertification-2009 (accessed 28 August 2014).

Theil, H., 1950. A rank invariant method of linear and polynomial regression analysis, Part 3. *Nederl. Akad. Wetensch. Proc*. 53: 397-1412.

Thompson, J.R. and Polet, G., 2000. Hydrology and land use in a Sahelian floodplain wetland. *Wetlands* 20: 639-659.

Vörösmarty, C.J., Mclntyre, P.B., Gessner, M.O., Dudgeon, D., Prusevich, A., Green, P., Glidden, S., Bunn, S.E., Sullivan, C.A., Liemann, C.R. and Davies, P.M., 2010. Global threats to human water security and river biodiversity. *Nature* 467: 555-561.

Welcomme, R.L. and Hagborg, D., 1977 Towards a model of a floodplain fish population and its fishery. *Environmental Biology of Fishes* 2: 7-24.

Westra, T. and De Wulf, R.R., 2009. Modelling yearly flooding extent of the Waza-Logone floodplain in northern Cameroon based on MODIS and rainfall data. *Int. J. Remote Sens*. 30: 5527-5548.

Westra, S., Fowler, H. J., Evans, J. P., Alexander, L. V., Berg, P., Johnson, F., Kendon, E. J., Lenderink, G. and Roberts, N. M. 2014. Future Changes to the Intensity and Frequency of Short-Duration Extreme Rainfall. *Reviews of Geophysics* 52, no. 3: 522–55. https://doi.org/10.1002/2014RG000464.

Yue, S., Pilon, P., Phinney, B. and Cavadias, G., 2002. The influence of Autocorrelation on the Ability to Detect Trend in Hydrological Series. *Hydrolo. Processes*, 16:1807-1829.

Supporting Material

Table S1: Comparison between instrumental observations and the value of the corresponding CRU grid. GHCN corresponds to Global Historical Climatology Network (https://www.ncdc.noaa.gov/data-access/land-based-station-data/land-based-datasets/global-historical-climatology-network-ghcn).

Name and Location	Grids	Length of record	Variable	Source	Years compared	Correlation (p-value)	Mean bias
MOUNDOU 8.62ºN, 16.07ºE	29	38 (1951-1996)	Temperature	GHCN	18	0.1	-0.08ºC
MAROUA-SALAK 10.45ºN, 14.25ºE	38	46 (1954-2000) 113 (1901-2013)	Temperature Rainfall	GHCN *in-situ*	25 113	0.42* 0.97*	-0.57ºC 49.5 mm
NGAOUNDERE 7.35ºN, 13.57ºE	7	49 (1951-2004) 40 (1951-1990)	Temperature Rainfall	GHCN Asmita	27 40	0.13 0.71*	1.31ºC -36.2 mm
BOUSSO 10.48ºN, 16.72ºE	42	24 (1955-1978)	Temperature	GHCN	18	0.66*	-0.7ºC
MEIGANGA 6.53ºN, 14.37ºE	1	21(1951-1981)	Temperature	GHCN	16	0.49*	0.2ºC
NDJAMENA 12.13ºN, 15.03ºE	54	60 (1949-2013)	Temperature	GHCN	23	0.77*	-0.27ºC
BAINAMAR 8.7ºN, 15.4ºE	27	41 (1951-1991)	Rainfall	GHCN	35	0.99*	-69.1 mm
KAIROUAL 9.5ºN, 15.2ºE	34	29 (1955-1992)	Rainfall	GHCN	23	0.53*	48.4 mm
GOUNOU-GAYA 9.6ºN, 15.5ºE	35	40 (1951-1993)	Rainfall	GHCN	35	0.95*	-108 mm
TIKEM 9.8ºN, 15ºE	34	36 (1955-1992)	Rainfall	GHCN	28	0.58*	9.2 mm
KELO 9.4ºN, 15.8ºE	31	43 (1946-1993)	Rainfall	GHCN	40	0.96*	4.7 mm
FIANG CFPA 9.9ºN, 15.2ºE	34	41 (1951-1992)	Rainfall	GHCN	33	0.95*	75.8 mm
TAUBORO 7.77ºN, 15.12ºE	18	48 (1955-2000)	Rainfall	*in-situ*	48	0.45*	-2.6 mm

Note: Asterisks (*) indicates correlation statistically significant at alpha = 0.1. The source of in-situ data is collected from administrative divison of Logone-Chari divison (received from our Cameroon colloborators).

Table S2: Regression equation of climatic parameters for Aw and BSh zones

Zones	Climatic Parameters	Entire Duration	Pre-1960	Post-1960
Aw	Rainfall	y=-0.2723x+1221.7 (R^2=0.01) (t=-0.798)	y = 2.2995x - 3216.2 (R^2=0.10)	y = -1.3856x + 3940.3 (R^2=0.04)
	Rainy Days	y = -0.0195x + 96.697 (R^2=0.02)	y = 0.0947x + 93.715 (R^2=0.13)	y = -0.0481x + 95.73 (R^2=0.03)
	Maximum Temperature	y=0.0022x+32.049 (R^2=0.03) (t=1.549)	y = 0.0059x + 20.665 (R^2=0.06)	y = 0.0148x + 2.7541 (R^2=0.28)
	Minimum Temperature	y = 0.0034x + 18.814 (R^2=0.07) (t=2.489*)	y = 0.0045x + 10.337 (R^2=0.04)	y = 0.0181x - 16.981 (R^2=0.40)
	PET	y = 0.0209x + 1471.5 (R^2=0.00)	y = 0.1702x + 1471.8 (R^2=0.04)	y = 0.4507x + 1458.3 (R^2=0.11)
BSh	Rainfall	y=-0.3217x+1355.3 (R^2=0.01) (t=1.022)	y = 1.9747x - 3064.5 (R^2=0.09)	y = 0.0076x + 685.82 (R^2=0.00)
	Rainy Days	y = -0.0135x + 48.169 (R^2=0.04)	y = 0.0496x + 46.62 (R^2=0.06)	y = -0.0022x + 46.628 (R2=0.00)
	Maximum Temperature	y = 0.006x + 34.75 (R^2=0.11) (t=3.369*)	y = -0.0109x + 56.123 (R^2=0.11)	y = 0.0262x - 16.94 (R^2=0.50)
	Minimum Temperature	y = 0.0054x + 20.373 (R^2=0.10) (t=3.19*)	y = -0.0119x + 43.644 (R^2=0.13)	y = 0.0234x - 25.743 (R^2=0.52)
	PET	y = 0.13x + 1873.2 (R^2=0.02)	y = -0.6429x + 1892.6 (R^2=0.25)	y = 0.9921x + 1852.5 (R^2=0.30)
*Note: Significance of trend line is indictaed by *.*				

Table S3: Annual MK/MMK –Z-statistics values for all parameters for the entire duration

Zones	Grids	Rainfall	Rainy Days	Minimum Temperature	Maximum Temperature	PET
	1	-0.923	-0.635	**3.667**	**2.182**	-0.156
	2	-0.566	-0.625	**3.708**	**2.281**	1.001
	3	-0.184	-0.749	**3.805**	**2.882**	0.475
	4	0.124	-1.303	**3.954**	**3.048**	**3.369**
	5	0.318	**-2.099**	**4.145**	**3.492**	**3.43**
	6	**-1.856**	-1.055	**3.419**	**2.081**	-0.482
	7	**-1.777**	-1.241	**3.651**	**2.284**	-1.02
	8	-1.308	-0.995	**3.8**	**2.358**	-0.367
	9	-0.849	-0.93	**3.582**	**2.54**	0.278
	10	-0.514	-0.71	**3.833**	**2.944**	1.307
	11	-0.102	-1.38	**4.049**	**3.163**	**1.716**
	12	0.402	**-1.873**	**4.292**	**3.552**	**3.49**
	13	0.313	**-2.253**	**4.216**	**3.715**	**3.796**
	14	**-1.868**	-1.181	**3.575**	**2.192**	0.052
	15	-1.437	-1.102	**3.686**	**2.112**	0.941
	16	-1.191	-0.958	**3.723**	**2.197**	-0.027
	17	-0.779	-0.759	**3.798**	**2.798**	1.047
	18	-0.457	-0.603	**4.382**	**3.426**	**3.495**
Aw	19	-0.094	-0.859	**4.402**	**3.607**	**3.364**
	20	0.288	-1.191	**4.337**	**3.645**	**3.478**
	21	-0.633	-1.618	**4.353**	**3.819**	**4.649**
	22	-0.844	-0.754	**3.88**	**2.746**	**2.269**
	23	-0.362	-0.752	**3.945**	**3.123**	**1.331**
	24	0.333	-0.94	**4.285**	**3.702**	**2.688**
	25	-0.186	-1.246	**4.41**	**3.928**	**3.058**
	26	-0.692	**-1.648**	**4.7**	**4.345**	**4.458**
	27	-0.223	-0.834	**3.866**	**3.058**	**2.84**
	28	-0.087	-1.127	**4.372**	**3.987**	**2.485**
	29	-0.184	-1.275	**4.428**	**3.281**	**3.459**
	30	-0.074	-1.556	**4.529**	**3.994**	**3.822**
	31	-0.203	-1.181	**4.155**	**3.613**	**1.845**
	32	-0.533	-1.213	**4.576**	**4.118**	**2.863**
	33	-0.444	-1.342	**4.763**	**4.025**	**3.044**
	34	-0.489	-1.112	**3.485**	**3.251**	**1.706**
	35	**-1.796**	-1.273	**4.349**	**4.13**	**2.615**
	36	-1.439	-1.323	**4.18**	**4.09**	**1.956**
	37	-1.151	-1.253	**4.222**	**3.97**	**2.063**

	38	**-1.792**	-1.399	**4.457**	**4.058**	**3.654**
	39	**-2.144**	-1.278	**4.82**	**4.241**	**3.353**
BSh	40	-0.417	-0.677	**3.065**	**3.079**	-0.129
	41	-0.439	-1.027	**3.407**	**3.197**	1.01
	42	-0.337	-1.06	**3.669**	**3.607**	**1.832**
	43	-1.221	-0.288	**3.028**	**2.898**	0.516
	44	-0.801	-0.496	**3.348**	**2.986**	0.668
	45	-1.067	-0.486	**3.59**	**2.933**	**1.655**
	46	**-1.712**	-1.519	**4.247**	**3.876**	**2.425**
	47	-1.608	-1.643	**4.237**	**3.731**	**3.105**
	48	**-2.223**	-1.402	**4.756**	**4.227**	**3.867**
	49	-0.357	-0.829	**4.152**	**3.444**	**2.565**
	50	-0.643	-1.598	**4.344**	**3.599**	**3.139**
	51	-0.429	-1.069	**4.229**	**3.499**	**3.538**
	52	0.082	-1.496	**4.616**	**3.447**	**2.185**
	53	0.298	-0.983	**4.496**	**3.888**	**2.739**
	54	-0.025	-1.385	**4.813**	**3.818**	**2.661**

Note: Negative and positive values indicate the decreasing and increasing trends, respectively. Bold values indicate the significant trends in the annual series for entire duration

Table S4: Magnitude of climatic parameter change during rainy and dry seasons. Values of the spatial minimum, maximum, and mean (in parentheses) are shown

	Parameter	**Rainfall**	**#Rainy Days**	**Max Temp**	**Min Temp**	**PET**
Zones	**Duration**	**mm**	**days**	**ºC**	**ºC**	**mm**
Rainy Season						
Aw	**1901-2013**	-98 to 39 (-14)	-3 to 0 (-1)	0.1 to 0.7 (0.4)	0.2 to 0.7 (0.4)	-10 to 10 (2)
	1901-1960	43 to 245 (142)	2 to 9 (5)	-0.5 to 0.6 (0.1)	-0.3 to 0.6 (0.2)	-5 to 5 (1)
	1961-2013	-129 to 51 (-53)	-5 to 0 (-2)	0.4 to 1.4 (0.8)	0.5 to 1.2 (0.8)	-1 to 28 (13)
BSh	**1901-2013**	-102 to 10 (-31)	-2 to 0 (-1)	0.4 to 1.1 (0.8)	0.5 to 0.9 (0.7)	-11 to 23 (9)
	1901-1960	29 to 160 (126)	2 to 5 (3)	-1.1 to -0.6 (-0.8)	-0.8 to -0.3 (-0.5)	-6 to 12 (5)
	1961-2013	-70 to 111 (3)	-2 to 2 (0)	0.9 to 1.9 (1.4)	0.9 to 1.3 (1.1)	11 to 45 (30)
Dry Season						
Aw	**1901-2013**	-34 to 0 (-12)	-1 to 0 (-1)	-0.2 to 0.3 (0.0)	0.1 to 0.3 (0.2)	-7 to 7 (0)
	1901-1960	-20 to 8 (-5)	-1 to 1 (0)	0.1 to 0.8 (0.5)	-0.2 to 0.7 (0.2)	-4 to 4 (0)
	1961-2013	-23 to 8 (-3)	0 to 1 (0)	0.6 to 1.1 (0.8)	1.2 to 1.6 (1.3)	2 to 19 (10)
BSh	**1901-2013**	-3 to 0 (-1)	0 to 0 (0)	-0.1 to 0.3 (0.1)	0.1 to 0.4 (0.2)	-13 to 7 (-1)
	1901-1960	-5 to 0 (-1)	0 to 1 (0)	-0.2 to 0.5 (0.1)	-0.6 to -0.1 (-0.4)	-7 to 4 (0)
	1961-2013	0 to 2 (1)	0 to 1 (0)	0.9 to 1.7 (1.3)	1.2 to 1.5 (1.3)	15 to 26 (20)

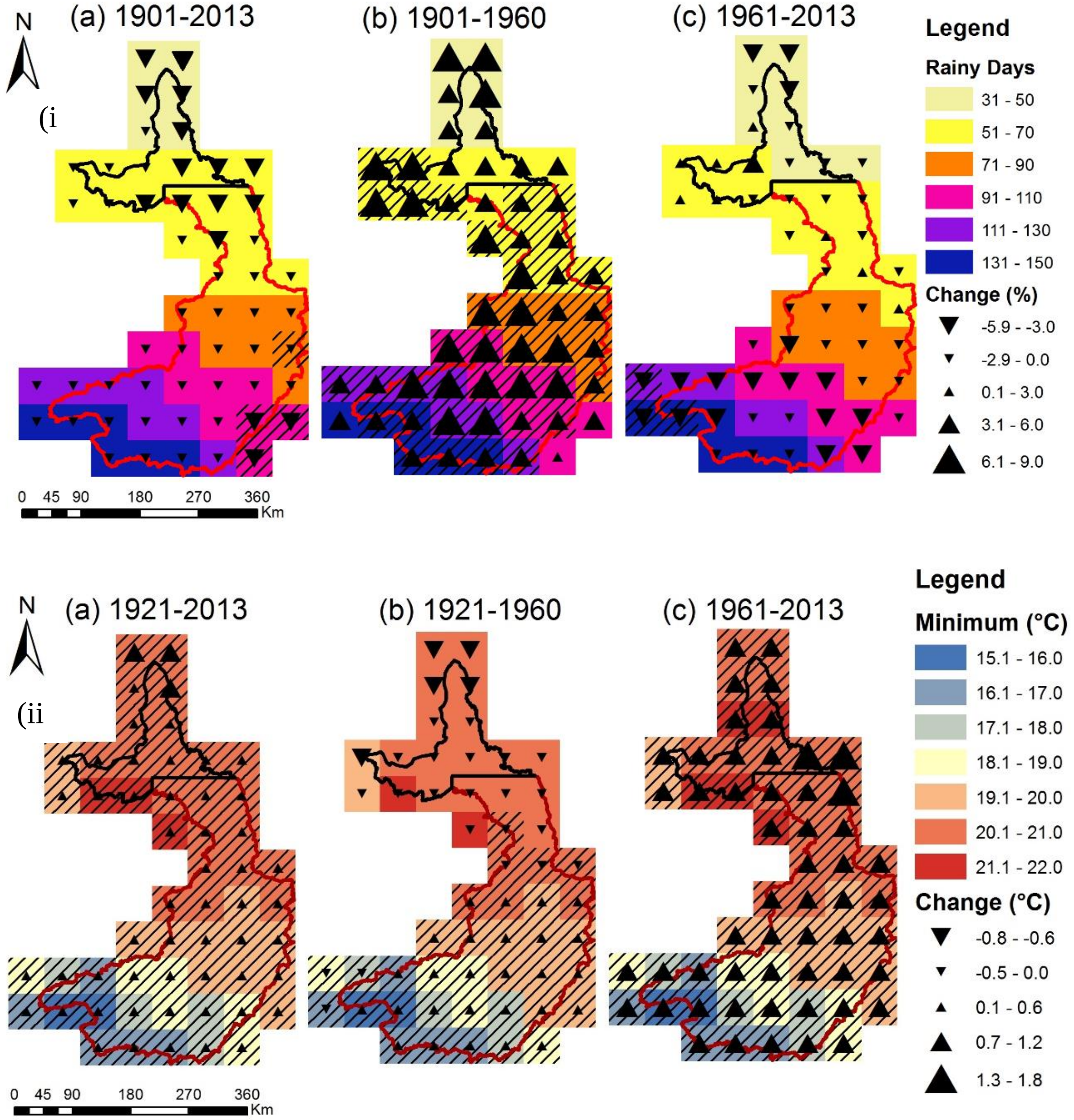

Fig S1. Spatial variability in annual (i) Rainy Days (first row) and (ii) Minimum Temperature (second row) over the basin during (a) 1901/1921-2013, (b) pre-1960 and (c) post-1960. Shaded grids indicate significant change. Red and black polygons indicate Aw and BSh climatic zones, respectively.

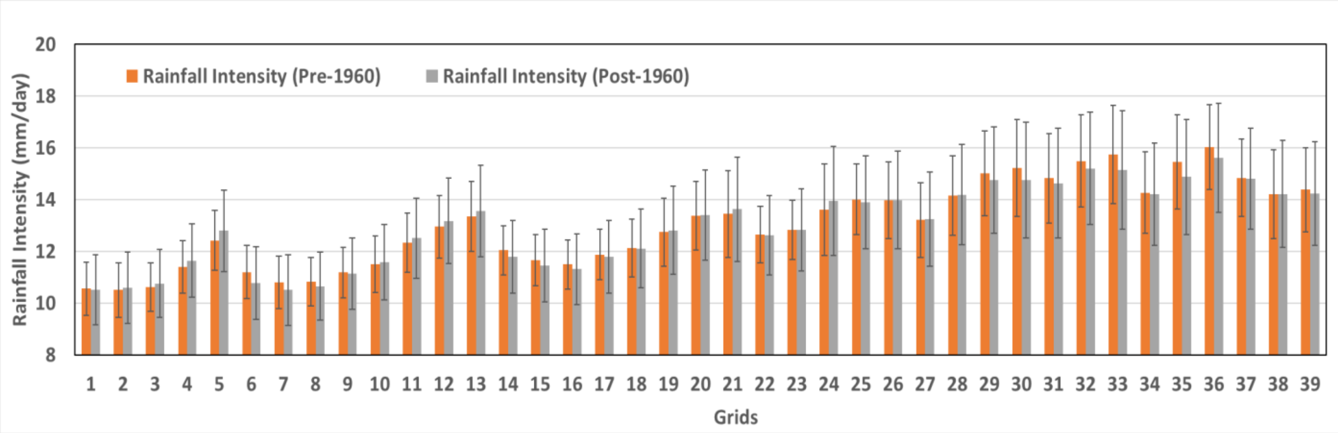

Fig S2. Rainfall intensity during pre-1960 compared with post-1960 across grids in the Aw zone (in watershed)

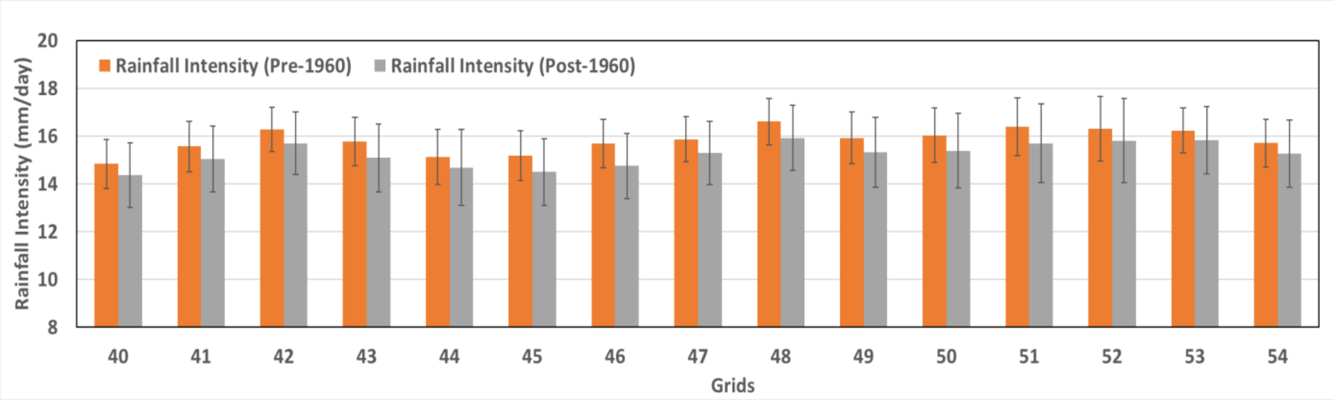

Fig S3. Rainfall intensity during pre-1960 compared with post-1960 across grids in the BSh zone (on floodplain)

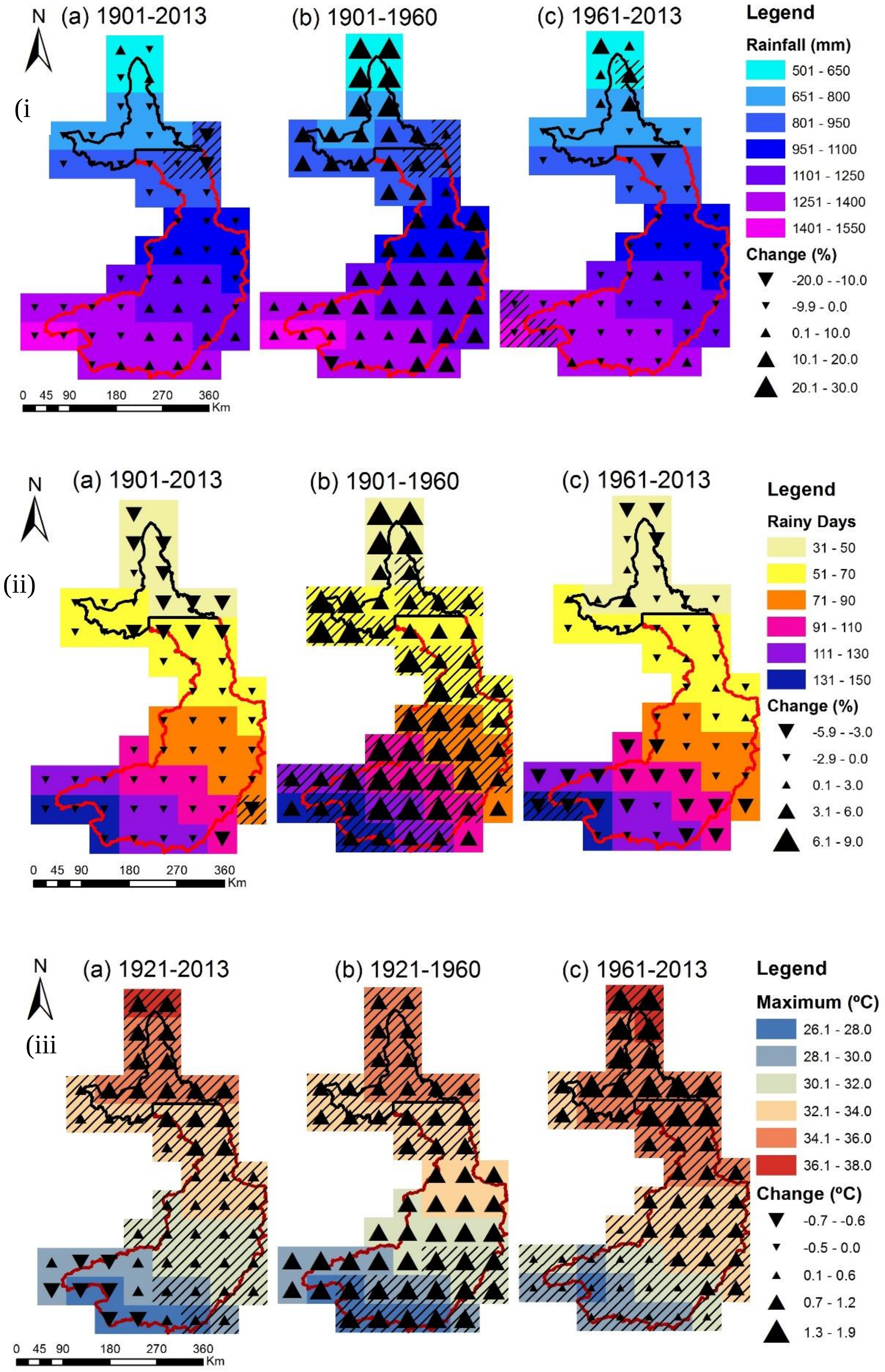
N
(a) 1901-2013
(b) 1901-1960
(c) 1961-2013
(i
Legend
Rainfall (mm)
501 - 650
651 - 800
801 - 950
951 - 1100
1101 - 1250
1251 - 1400
1401 - 1550
Change (%)
-20.0 - -10.0
-9.9 - 0.0
0.1 - 10.0
10.1 - 20.0
20.1 - 30.0
0 45 90 180 270 360
Km
N
(a) 1901-2013
(b) 1901-1960
(c) 1961-2013
(ii)
Legend
Rainy Days
31 - 50
51 - 70
71 - 90
91 - 110
111 - 130
131 - 150
Change (%)
-5.9 - -3.0
-2.9 - 0.0
0.1 - 3.0
3.1 - 6.0
6.1 - 9.0
0 45 90 180 270 360
Km
N
(a) 1921-2013
(b) 1921-1960
(c) 1961-2013
(iii
Legend
Maximum (ºC)
26.1 - 28.0
28.1 - 30.0
30.1 - 32.0
32.1 - 34.0
34.1 - 36.0
36.1 - 38.0
Change (ºC)
-0.7 - -0.6
-0.5 - 0.0
0.1 - 0.6
0.7 - 1.2
1.3 - 1.9
0 45 90 180 270 360
Km

(iv

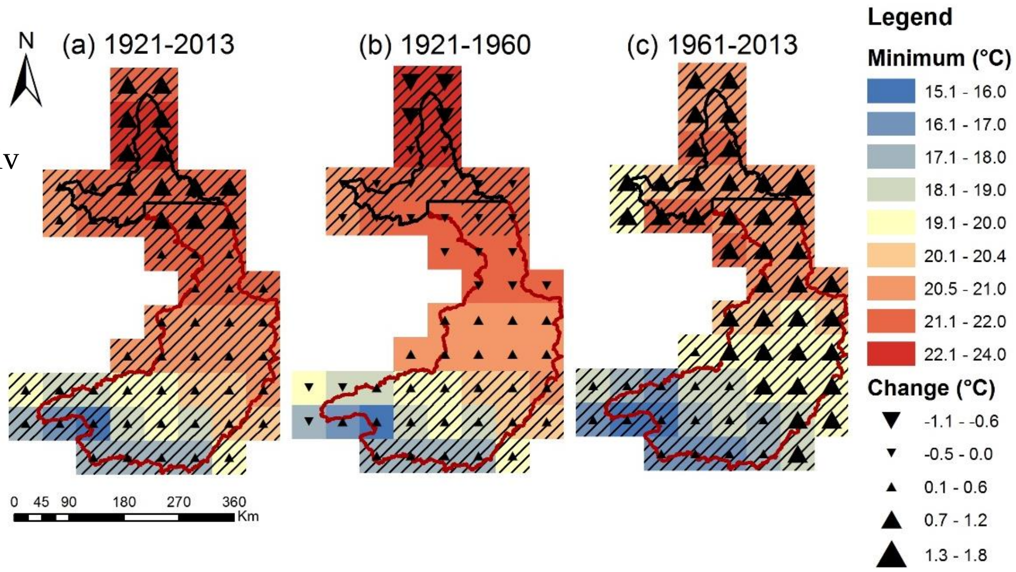

(v

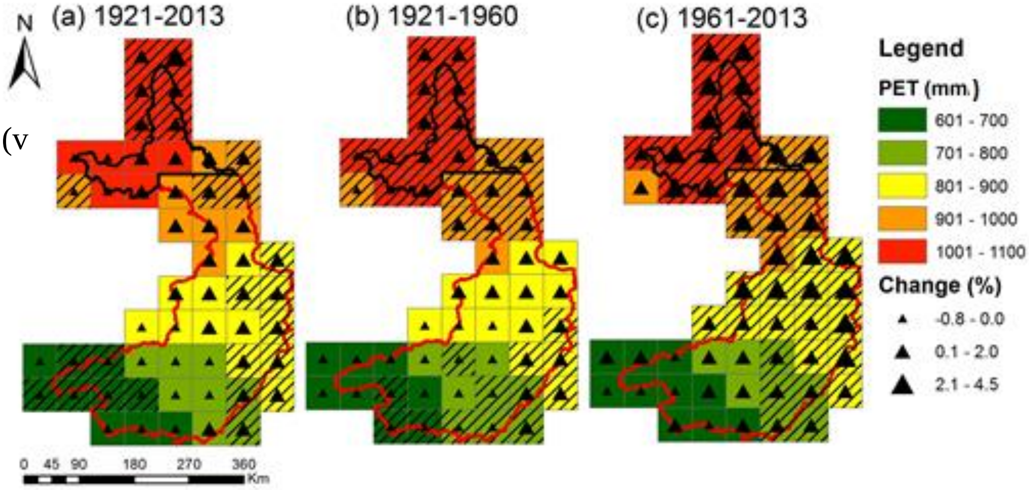

Fig S4. Spatial variability of rainy season (i) Rainfall (first row), (ii) Rainy Days (second row), (iii) Maximum Temperature (third row), (iv) Minimum Temperature (fourth row) and (v) PET (fifth row) over the basin during (a) 1901/1921-2013, (b) pre-1960 and (c) post-1960. Shaded grids indicate significant change. Red and black polygons indicate Aw and BSh climatic zones, respectively.